



## REINFORCED CONCRETE MASONRY PILASTER DESIGN AIDS

Paul G. Gurley<sup>1</sup> and Russell H. Brown<sup>2</sup>

### ABSTRACT

Reinforced masonry pilasters are often used in masonry construction to resist concentrated loads or to serve as vertical reaction beams for walls spanning horizontally. Their use in large warehouse buildings is both practical and economical. Efficient design of reinforced masonry pilasters with combined axial load and bending requires either a computer solution or the use of graphical or tabular load-moment interaction diagrams. This paper discusses the development of load-moment interaction diagrams for reinforced concrete masonry pilasters and presents several example diagrams.

### INTRODUCTION

Masonry pilasters are column or thickened wall elements built integrally with and forming part of a masonry wall. They are designed to provide lateral support for walls subjected to lateral loads such as those caused by wind or seismic forces, and to carry the vertical loads transferred from beams and trusses due to the presence of roof and floor systems and/or overhead bridge cranes. The cross sectional view of a typical pilaster is shown in Fig. 1. Analysis and design of such a structural element is very cumbersome, realistically requiring either a computer solution or a graphical solution similar to the interaction diagrams used for reinforced masonry or concrete columns. Approximating the capacity as if it were equivalent to a column without

---

<sup>1</sup> Product Engineer, Metromont Materials Corporation, P.O. Box 1292, Spartanburg, SC, USA 29304 (M.E.C.E., Clemson University, 1993)

<sup>2</sup> Professor and Head, Civil Engineering Department, Clemson University, Clemson, SC, USA 29634-0911

the wall flanges was expected to be unduly conservative. Hence, the authors undertook the development of design aids for pilasters.

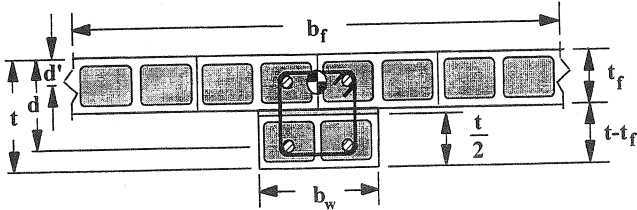


Figure 1 - Cross sectional view of a typical pilaster.

The number of possible variables for the design aids, such as concrete block sizes and configurations, steel area, masonry strength, cell grouting, and lateral confinement of longitudinal reinforcement would have resulted in hundreds of graphs. Consultation with the engineering staff of the National Concrete Masonry Association (NCMA) provided valuable guidance based on their knowledge of the national trends in reinforced concrete masonry pilaster design and construction. The authors also considered using a non-dimensionalized form of the diagrams. However, for the T-shaped pilasters, non-dimensionalization did not appear to be as useful as in the case for symmetrical sections such as columns. Following much experimentation and observation of various diagram prototypes the decision was made to assimilate the families of interaction diagrams for 8 inch walls (nominal) by the hierarchy (shown in Table 1) based on steel confinement, masonry strength and pilaster size (nominal):

TABLE 1

Longitudinal Steel Laterally Tied		Longitudinal Steel NOT Laterally Tied	
$f'_m$	$t \times b_w$	$f'_m$	$t \times b_w$
1500 psi	16 x 16	1500 psi	16 x 16
	16 x 24		16 x 24
	24 x 16		24 x 16
2500 psi	16 x 16	2500 psi	16 x 16
	16 x 24		16 x 24
	24 x 16		24 x 16

The major classifications of longitudinal steel tied or not tied were chosen to be the primary distinguishing characteristic because the *Building Code Requirements for Masonry Structures* (ACI 530 - 92 / ASCE 5 - 92 / TMS 402 - 92) does not permit an allowable stress for steel in compression unless it is laterally tied.

Pilasters may be constructed so that they may be either T - shaped, L - shaped or column shaped as shown in Fig. 2. Each of these configurations results in a drastically different shape of the resulting design aid as illustrated by the three families of curves in Fig. 3. The resulting asymmetrical shape may be a consequence of placing an expansion joint immediately adjacent to the column portion of the pilaster or of placing a pilaster at the end of a wall. This condition sets the effective flange width equal to six times the wall thickness ( $t_f$ ) plus the pilaster web thickness ( $b_w$ ). The largest outer family of curves represent the fully effective T-shape of the pilaster (Fig. 2(a) and Fig. 3). The effective flange width ( $b_f$ ) is set equal to twelve times the wall thickness ( $t_f$ ) plus the pilaster web thickness ( $b_w$ ).

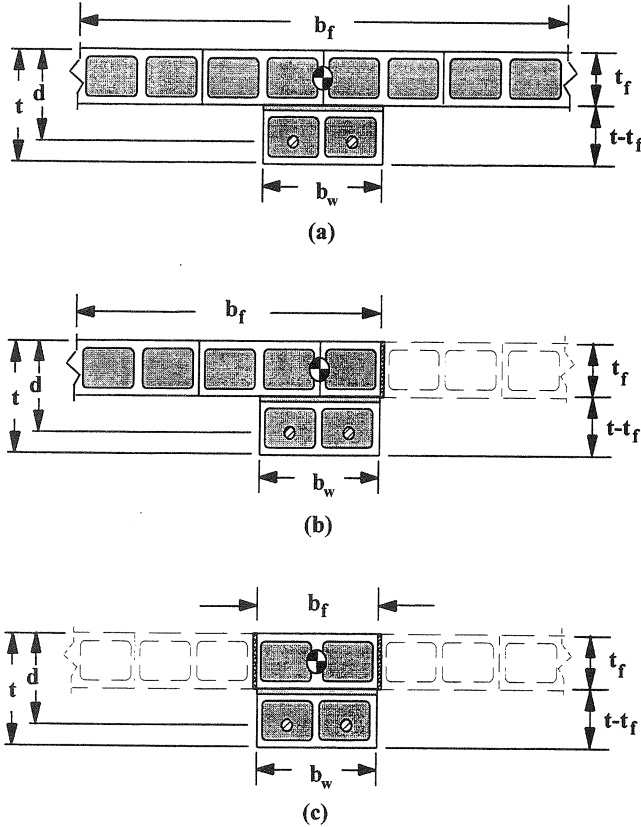


Figure 2 - Illustration of (a) Effective width  $b_f = 12t_f + b_w$  (b) Effective width  $b_f = 6t_f + b_w$  (c) Effective width  $b_f = b_w$  for solidly grouted walls.



There are two general cases presented for the partially grouted wall diagrams. Ref. 1 (Gurley, 1993) presents twelve design aids, similar to Fig. 3, which include all of the variables shown in Table 1 for fully grouted construction. Since the wall portion may only be partially grouted, if at all, twelve additional curves are presented in Ref. 1 for partially grouted construction. Fig. 4 shows the contrast between full and partial grout for T - shaped sections. Comparison of the two families of curves shows the substantial increase in axial load carrying capacity achieved by solidly grouting the cells in the wall for the entire effective flange width, as compared to solidly grouting only the central column portion and securing the masonry in the wall with faceshell bedding only.

Finally, each family of curves in Fig. 3 is comprised of five particular areas of steel reinforcement, and each curve is labeled by reinforcing steel bar size designation for ease of use. The pilasters with a sixteen inch nominal core width ( $b_w = 16''$ ) have one bar in each of the two exterior cells per face. The pilasters with a twenty four inch nominal core width ( $b_w = 24''$ ) have one bar in each of the three exterior cells per face.

### ACI 530 CODE REQUIREMENTS

The load interaction diagrams in Ref. 1 (Gurley, 1993) were developed in accordance with existing criteria set forth for reinforced concrete masonry walls, columns, and pilasters in the masonry code (ACI 530-92). The modulus of elasticity ( $E_m$ ) of the masonry was determined by interpolation for  $f_m$  values of 1500 and 2500 p.s.i. The compressive strength of the masonry ( $f_m$ ) was converted to the compressive strength of the individual concrete masonry units (cmu) with type M or S mortar from Specification Table 1.6.2.2 (ACI 530.1-92). This value was then used for the interpolation from Table 1.6.2.2 to determine the elastic modulus of the masonry,  $E_m$ , from which the modular ratio,  $n$ , could be determined for transformed section analysis. The special code requirements for pilasters are given in Section 5.10. The criteria for design of the wall intersection are covered in Section 5.13.4.2. The lateral reinforcement requirements are given in Section 5.9.1.6. The requirements for the stress computations are given in Section 5.13.1. The allowable stresses in the steel reinforcement were taken from Section 7.2. The only grade of steel used to develop these diagrams was Grade 60, therefore the allowable stress for steel in tension and compression was 24000 psi from Sections 7.2.1.1 and 7.2.1.2, respectively. The allowable stress for the masonry in compression was taken from Section 7.3.1.2.

$$F_b = \frac{1}{3} f'_m$$

The placement limits for the reinforcement are given in Section 8.3. The requirements for protection of reinforcement are specified in Section 8.4. When

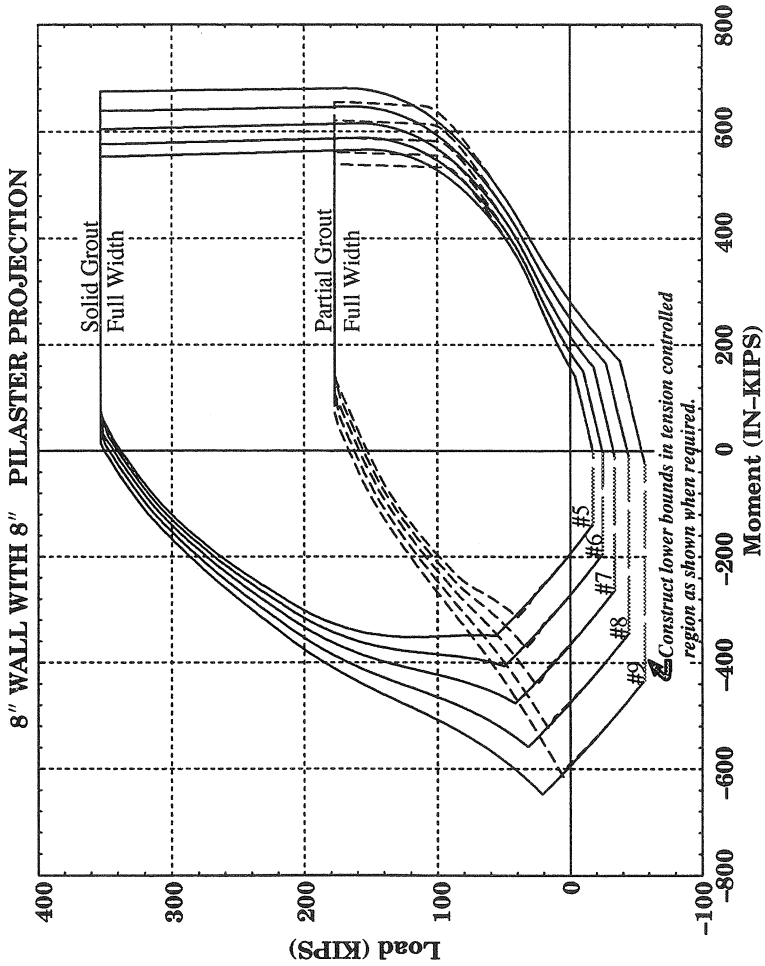


Fig. 4 Comparison of Partially and Fully Grouted Pilaster Interaction Diagrams

generating the diagrams, the effective depth,  $d$ , was calculated by subtracting the required two inches of cover to the outside of the vertical reinforcement and an additional one half of the particular bar diameter from the exterior of the masonry block. By doing this, the distance between reinforcing bars was maximized, and consequently the size of the moment couple, while maintaining cover requirements. This leaves a 1/2" space between a #2 tie and the inside cell wall, a 3/8" space between a #3 tie and the inside cell wall, and a 1/4" clearance between a #4 tie and the inside cell wall. Therefore, in accordance with the placement requirements set forth in Section 8.3, these diagrams are valid for #2, #3, and #4 ties when used in conjunction with grout classified as FINE grout as per ASTM C 476 (ASTM C-476-87). If grout classified as COARSE grout as per ASTM C 476 is to be used with ties larger than #2, the vertical reinforcement would have to be moved an additional 1/8" to 1/4" from the inside cell wall to comply with the placement requirements, which would subsequently reduce the magnitude of the moment couple. This action would cause the design aids to yield slightly *unconservative* results.

The load interaction diagrams in Fig. 3 and Ref. 1 are developed for a zero height wall. By setting the height equal to zero, the slenderness effects of the code requirements do not affect the maximum allowable axial load capacity. This means that the maximum allowable axial stress must be determined for a particular ratio of wall height to the radius of gyration. The allowable stress is then multiplied by the net cross sectional area of the pilaster to determine the height of the upper bound for the load interaction diagram under consideration. This upper bound should be plotted as a straight line which is normal to the vertical axis at the calculated load. To attempt to eliminate the need for as many repetitive calculations as possible, allowable axial loads for even heights of walls have been calculated in accordance with code Section 7.3 equations (7-1) and (7-2) and are presented in Table 2. A more detailed set of tables appears in Ref. 1 (Gurley, 1993) tables 3-8 through 3-12.

$$F_a = \frac{1}{4} f'_m \left[ 1 - \left( \frac{h}{140r} \right)^2 \right] \quad \text{For } h/r < 99 \quad (\text{Code eqn. 7-1})$$

$$F_a = \frac{1}{4} f'_m \left( \frac{70r}{h} \right)^2 \quad \text{For } h/r \geq 99 \quad (\text{Code eqn. 7-2})$$

- Where  $F_a$  = Maximum allowable compressive stress from an axial load (p.s.i.)  
 $f'_m$  = Specified compressive strength of masonry (k.s.i. or p.s.i.)  
 $h$  = Maximum unsupported height of the pilaster (in.)  
 $r$  = Minimum radius of gyration (in.)

These tabulated allowable compressive stresses represent the upper limit of the pilaster axial load capacity, when multiplied by the cross sectional area of the pilaster. The axial loads calculated by either of these two equations will always

control over the maximum axial load shown on the design aids in Ref. 1 (Gurley, 1993).

**TABLE 2 - ALLOWABLE AXIAL CAPACITY**

Longitudinal Steel *NOT* Laterally Tied

$f_m = 1500$  p.s.i.  
 $F_s = 24000$  p.s.i.

Class.	$I_c$ (in <sup>4</sup> )	A (in <sup>2</sup> )	r (in)	$P_{max}$ (Kip)				
				8 (ft)	12 (ft)	16 (ft)	20 (ft)	24 (ft)
<b>16 x 16"</b>								
$b_f = 12t_f + b_w$	11148	942	3.440	339	322	297	265	227
$b_f = 6t_f + b_w$	8864	593	3.866	215	207	194	179	159
$b_f = b_w$	4877	244	4.469	89	87	83	78	72
*pg $12t_f + b_w$	9213	473	4.414	173	168	160	151	139
pg $6t_f + b_w$	7391	359	4.541	131	128	122	115	107
<b>16 x 24"</b>								
$b_f = 12t_f + b_w$	14614	1067	3.701	386	369	345	314	276
$b_f = 6t_f + b_w$	11932	718	4.077	262	252	239	222	201
$b_f = b_w$	7374	369	4.469	135	131	125	118	109
pg $12t_f + b_w$	12126	598	4.503	219	213	203	192	177
pg $6t_f + b_w$	10085	484	4.567	177	172	165	156	145
<b>24 x 16"</b>								
$b_f = 12t_f + b_w$	31241	1067	5.411	394	386	374	360	342
$b_f = 6t_f + b_w$	25580	718	5.969	266	261	255	247	237
$b_f = b_w$	12412	369	5.799	136	134	131	126	121
pg $12t_f + b_w$	28564	598	6.912	222	219	215	210	204
pg $6t_f + b_w$	23936	484	7.036	180	177	174	171	166

\*pg refers to faceshell mortar bedding only in the overhanging wall flanges.

**GRAPHIC EXAMPLES OF INTERESTING RELATIONSHIPS**

Before the format for the hierarchy of curves was decided, many different example graphs were plotted to study trends and relationships between various parameters. Some provided new insights into the behavior of pilasters and are the basis on which the final versions of the pilaster design aids of Ref. 1 (Gurley, 1993) are developed. Others were not deemed to be useful as design aids, but do show interesting relationships. One such graph, Fig. 5, shows a load interaction envelope developed with respect to the elastic centroid of a pilaster superimposed over the load interaction envelope developed with respect to the center of the wall flange of the same pilaster. The graph shows one of the most crucial relationships from which all of the load interaction diagrams were developed. Typical interaction diagrams are constructed for use with symmetrically shaped columns with symmetrical reinforcement. In the case of symmetrical columns, the geometric centroid coincides with the elastic centroid, which is the point on the cross section



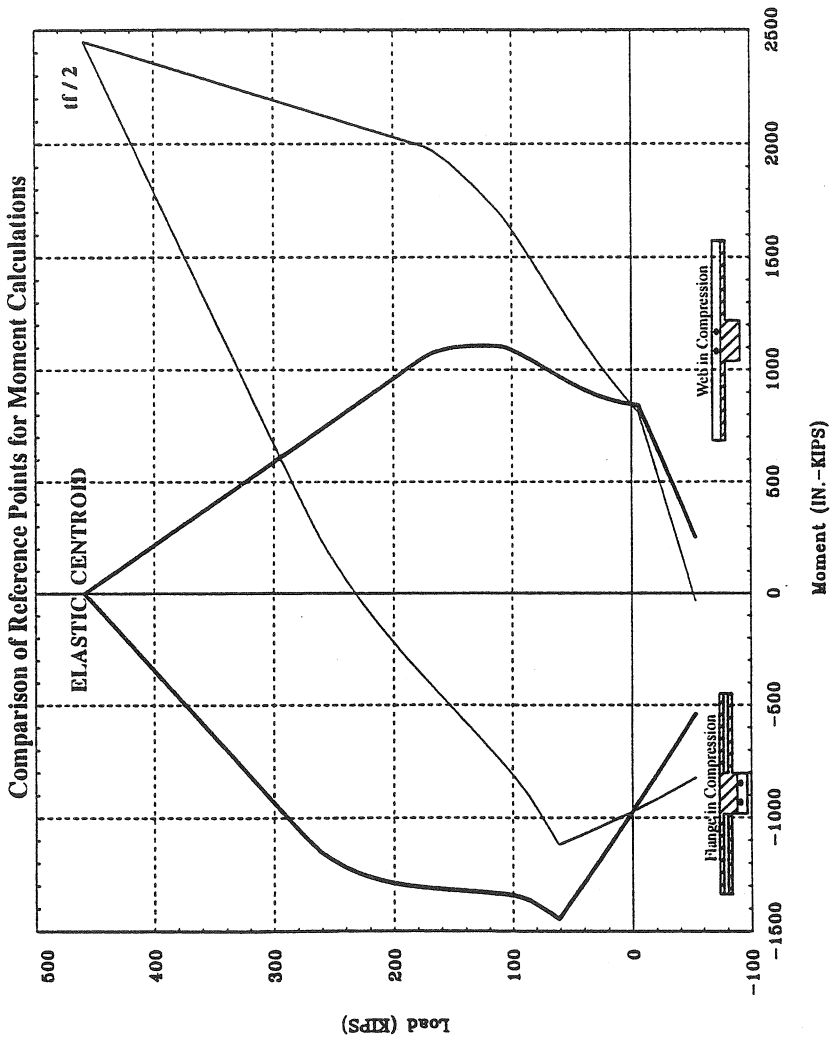


Fig. 5 Comparison of Reference Points for Moment Calculations

through which the maximum axial load will act to produce uniform strain across the section. This condition of uniform strain means that there will be zero net moment produced from this loading. The elastic centroid, Fig. 5, is typically chosen as a reference point for constructing load interaction diagrams because the maximum load will coincide to the zero net moment condition and plot directly on the vertical axis. The problem with using the elastic centroid for the reference point for an asymmetrically shaped pilaster is the need for repeating the somewhat laborious series of calculations each time a change in pilaster configuration, material strength, or steel reinforcement is tried. Because the ability of the wall to span horizontally will usually govern the pilaster spacing, the thickness of the wall will already be known by the time the actual pilaster size and reinforcement configuration are selected. Since the center of the wall will most likely remain constant throughout the pilaster design process, it appeared to be the logical choice for a reference point. The resulting load interaction curve is shown on the graph to be skewed to the right, even at the point of maximum axial load. The curve is skewed because there is some amount of eccentricity between the elastic centroid and the reference point at the center of the wall. The graph shows that the axial load information plots at the same elevations on either curve, but the moment values are translated to the right. Although the curves do not look like the typical interaction curves, the intent was to make them as "user friendly" as possible.

### **IMPORTANT LOCATIONS ON THE CROSS SECTION**

The families of load - moment interaction diagrams were developed using a spreadsheet program on a workstation. Two separate primary cases were identified during the initial analysis and development stages. The first case was labeled "Case A", and corresponds to the masonry of the pilaster, or "web", being placed initially in compression. The second case was labeled "Case B", and corresponds to the masonry of the wall, or "flange", being placed initially in compression. For each separate case under consideration, the neutral axis was placed near the extreme limit of the cross section, and the magnitudes of the resultant forces and subsequent moment couples were calculated using basic mechanics. This process was then repeated after increasing the depth to the neutral axis, "kd", by some small increment. Each subsequent row of the spreadsheet was used to recalculate all of the information each time "kd" was increased. Several critical regions of the pilaster cross section were identified which would require the equilibrium equations to be modified as the neutral axis was passed through them. To better illustrate the processes involved, the development of the equilibrium equations for Case B, where the neutral axis was initially placed adjacent to the exterior of the wall, will be presented in detail. From Figure 6, several critical regions and control points were identified for solidly grouted pilasters with laterally tied steel.

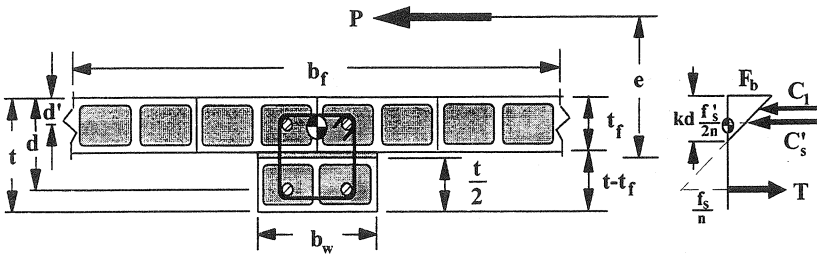


Figure 6 - Region 1 - Neutral axis between  $d'$  and  $t_f$  ( $F_b$  controls).

### The Regions

1. The neutral axis depth,  $kd$ , is between  $d'$  and  $t_f$ . The stress wedge for the masonry in compression in the wall is triangular. The modular ratio used for compression steel is "2n" to account for creep.
2. The neutral axis depth,  $kd$ , is between  $t_f$  and  $d$  and the stress wedge for the wall (to a depth  $t_f$ ) becomes trapezoidal. The stress wedge for the material below the wall is triangular.
3. The neutral axis depth,  $kd$ , is between  $d$  and  $t$  and the tension steel is now in compression.
4. The masonry stress at the interior face of the pilaster is incrementally increased to calculate the stresses in the steel and masonry from the stress diagram by the principle of similar triangles. The basic algorithm for incrementing the neutral axis is changed in this region to economize on the number of steps required to reach the final step.

### The Control Points

1. The neutral axis depth,  $kd$ , is located at the distance  $t$ . The entire cross section is now in compression.
2. The cross section experiences uniform strain, and hence, uniform compressive stress. This corresponds to the maximum load acting through the elastic centroid of the cross section.

The resulting forces are substituted into the horizontal equilibrium equation:

$$P = C_1 + C'_s - T$$

The resulting forces are multiplied by their corresponding moment arms with respect to the point  $t_f/2$  :

$$\sum M_{t_f/2} = C_1 \left( \frac{t_f}{2} - \frac{kd}{3} \right) + C'_s \left( \frac{t_f}{2} - d' \right) + T \left( d - \frac{t_f}{2} \right)$$

The eccentricity is calculated as :

$$e_{t_f/2} = \frac{M_{t_f/2}}{P}$$

The flat portion at the top of each of the three families of curves in Fig. 3 illustrates a change in the controlling allowable stress from  $1/3 f_m$  to  $1/4 f_m$ .

## CONCLUSIONS

It is the intent of the authors that the load interaction diagrams in Ref. 1 (Gurley, 1993) will prove useful as design aids for reinforced concrete masonry pilaster design. The diagrams show a significant increase in economy that results from consideration of the wall flanges. These design aids show a considerable increase in axial capacity and "Case B" bending moment capacity from considering even one flange projection adjacent to the column portion of the pilaster. Additionally, the diagrams for laterally tied pilasters show the marked increase in "Case A" moment capacity achieved when the longitudinal reinforcement is laterally tied and the pilaster web is placed in compression. The increased axial and bending moment capacities realized by including the contributions of the wall flanges could result in greater pilaster spacing and consequently fewer pilasters. Fewer pilasters would result in a decrease in material costs and, perhaps more importantly, a noticeable decrease in labor costs.

## CONVERSION FACTORS

1 square inch = 645.2 square mm	1 p.s.i.=6894.8 Pascals	1 inch-kip=16.308 KN-m
1 pound force=4.448 newtons	1 inch=25.4 mm	1 kip=1000pounds=4448 newtons

## REFERENCES

1. Gurley, Paul G. *The Development of Load Interaction Diagrams for Reinforced Concrete Masonry Pilaster Design*, Special Project Report, Clemson Univ., Clemson, SC, 1993. (Copies are available through The Masonry Society, 3775 Iris Avenue, Suite 6, Boulder, CO USA 80301. Phone (303) 939-9700. Fax (303) 541-9215.)
2. *Building Code Requirements for Masonry Structures* (ACI 530-92/ASCE 5-92/TMS 402-92), American Concrete Institute, Detroit, Michigan, American Society of Civil Engineers, New York, New York, The Masonry Society, Boulder, Colorado, 1992.
3. American Society for Testing and Materials, ASTM C-476, "Standard Specification for Grout for Masonry," *Annual Book of Standards*, Volume 4.05, Philadelphia, Pennsylvania, 1987.
4. *Specifications for Masonry Structures* (ACI 530.1-92/ASCE 6-92/TMS 602-92), American Concrete Institute, Detroit, Michigan, American Society of Civil Engineers, New York, New York, The Masonry Society, Boulder, Colorado, 1992.